PROCEEDINGS OF THE SMART ROCKETS PROJECT: DESIGN DEVELOPMENT AND FIRST MEASUREMENT RESULTS OF A 500 N LOX/ETHANOL COMBUSTION CHAMBER

J. Sieder[1], C. Bach[2], M. Nürmberger[3], N. Voigt[4], O. Przybilski[5] and M. Tajmar[6]

Institute of Aerospace Engineering, TU Dresden, 01062 Dresden, Germany

Abstract

The SMART Rocket Project commits itself to the development and flight of a liquid propelled sounding rocket. The envisaged LOX/Ethanol rocket engine is unique within the DLR STERN student education programme. First steps towards the engine development are presented, starting with first concepts. The test bench needed for the characterization of the engine is described, followed by test combustion chambers for material and load analyses. First characterization tests were conducted and are presented. The launch of the rocket is planned for 2016.

1. INTRODUCTION

The SMART Rockets Project[7] (SRP) is a student education programme at the Technische Universität Dresden (TU Dresden) with the ambitious goal of developing, testing and flying a liquid propelled sounding rocket using liquid oxygen (LOX) and ethanol (Eth). This project is embedded within the nationwide education programme Studentische Experimentalraketen (STERN), initiated and conducted by the German Space Administration (DLR) and funded by the Federal Ministery of Economics and Technology (BMWi). The main purpose of the STERN programme is the promotion of young professionals for launcher systems and a practical education of students in the field of aerospace engineering.[1]

While most universities use a hybrid engine with solid fuel and liquid oxidants, a solid or a hot water engine, the use of solely liquid propellants is one-of-a-kind within the STERN programme. The decision for ethanol and liquid oxygen presents a singular opportunity for our students to obtain experience in the handling of cryogenic fuels as well as the possibility of influencing the combustion by simply thinning the ethanol with water.

The official beginning of the SRP was in August 2012, despite the fact that a lot of preparatory work has been done by students in many theses and scientific research work. The current state of the project is the final definition phase C, in which the design of the rocket and the supporting peripherals are finalized and first essential tests are conducted. The scope of this paper is the development of the SRP rocket engine and the presentation of our first test results. A complete overview of the project can be obtained in the parallel work of Bach et al in [2].

For the development and testing of the combustion chamber and the fluid system a test bench has been manufactured, which is described in chapter 2. Furthermore, this chapter displays the measured values and the derivation of essential performance data. The combustion chamber design itself is presented in chapter 3. Three different test combustion chamber types are used for obtaining experience in material behaviour and additional sensors are used for a full characterization of the combustion chamber design. The upcoming chapter 4 presents the results of the recently conducted experiments. It begins with flow rate tests of the coaxial swirl injector, covers open combustion, igniter system and first combustion chamber tests. Chapter 5 finalizes this paper and gives an outreach about the upcoming test scenarios of our combustion chamber development.

2. TEST BENCH

In order to develop a rocket engine for the SRP, a test bench has been built. Its purpose is not only the verification and validation of the rockets propulsion system. Besides the optimization of system parameters, the preparation, conduction and also the documentation of test procedures are of high interest for the student project. This chapter will give an overview of the test bench setup, the used sensors to acquire the required measurement data and the evaluation of the data obtained.

2.1. Test Bench Setup

The test bench is an accurate functional model of the rockets propulsion system. It consists basically of the LOX and ethanol pipelines, a nitrogen pressurization system, an engine rack holding the injector plate and injector, and

[1] Dipl.-Ing. Jan Sieder is Ph.D. student and administrator of the SRP
[2] Dipl.-Ing. Christian Bach is Ph.D. student and administrator of the SRP
[3] Dipl.-Ing. Maximilian Nürmberger is research assistant within the SRP
[4] Dipl.-Ing. Niklas Voigt is research assistant within the SRP
[5] Dr.-Ing. Olaf Przybilski is member of the scientific staff, the initiator and the manager of the SRP
[6] Prof. Dr. Martin Tajmar is head of the Space Systems Chair and leader of the research group “Space Propulsion and new Concepts”
[7] Ref.-Nr. 50 RL 1256

a control and sensor system. The latter includes a control box, the sensor system and the control computer.

Just as later in the rocket, pressurized nitrogen is used to drive the propellants out of their tanks. The nitrogen is provided in a customary gas cylinder and flows through a pressure reducing valve to the control box, where the mass flow is divided into three different pipelines: the LOX tank pressurization pipeline, the ethanol pressurization pipeline, the pressurization pipelines for the pneumatic main control valves and the flushing pipes.

The LOX and ethanol pipelines are constructed very similar to each other. Both start from an aluminium tank containing the liquid. On the upper side of those tanks an adapter is installed, which allows the mounting of different controls and instruments. By now there are a connection for the pressurization, which is secured with a back-pressure valve, a pressure sensor, a manometer and a pressure control valve. The pressure control valve on the ethanol tank can be opened manually. On the LOX tank, there is an additional bleed valve and a rupture disk installed. On the bottom side of both tanks, the fluid track is mounted. They both contain a filter, a pneumatic main valve, a back-pressure valve and of course sensors for measuring the mass flow and pressure.

Both pipelines also contain an emergency system. Both tanks can be depressurized and drained with the help of pneumatic valves and both fluid tracks can be flushed with nitrogen. Therefore a nitrogen pipe with a back-pressure valve is connected to the fluid tracks.

Following the fluid tracks, the injector plate holding the injector is mounted to the engine rack. Here, the injector plate is the connecting piece between fluid tracks and combustion chamber. The engine rack is designed with a main focus on variability. It is constructed to enable the testing of different engines in a thrust range from 100 to at least 3000 N by using elementary lever principles.

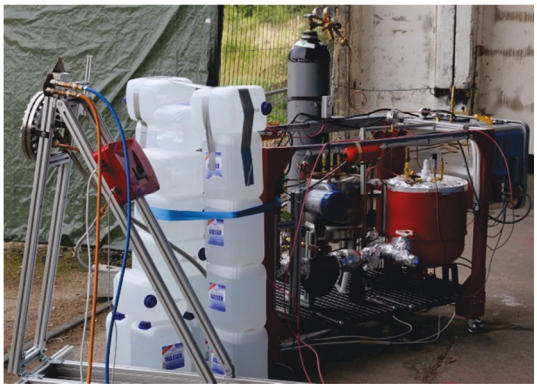

FIG 1. Test Bench and Engine Rack (front)

2.2. Sensor Setup

The test bench contains a variety of different sensors in order to acquire measurement data and monitor the test bench while performing tests. Those sensors are: pressure sensors, temperature sensors, a volume flow sensor for ethanol, a Coriolis sensor for LOX and a force sensor. FIG 2 shows a scheme of the test bench and the position of the used sensors.

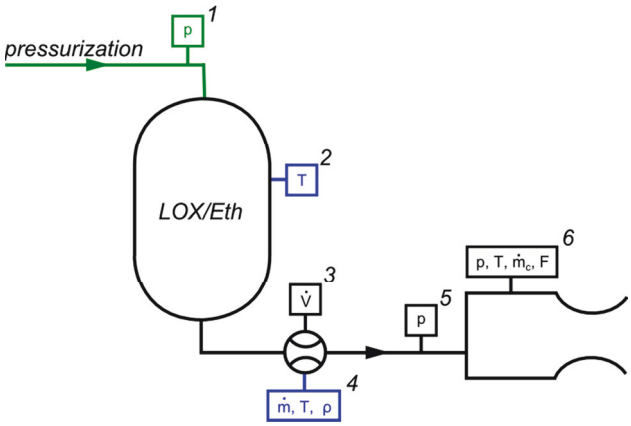

FIG 2. Sensor positions within the test bench

Because the LOX and ethanol pipelines are constructed very similar to each other, this scheme is simplified and shows only one pipeline. The pressure is measured at three positions: on top of the LOX/Ethanol tank in order to determine the tank pressure (1), within the fluid tracks shortly before the injector (5) and within the combustion chamber (6). Only on the LOX pipeline, there is a temperature sensor on the outside of the aluminium tank but underneath the insulation (2). In the ethanol track, the volume flow is measured (3), whereas the Coriolis sensor within the LOX track records mass flow, temperature and density (4). With the engine rack, it is possible to determine the thrust of the used combustion chamber (6). The test combustion chamber, shown in chapter 3.3.3, offers the possibility to acquire the chamber wall temperature as well as the temperature of the used coolant and its mass flow (6).

The sensors are connected to the control box. Here, their signals are read by an NI-DAQ system which is connected to the control computer. On the control computer a LabVIEW program evaluates the data, displays the variables while running a test and also saves them into a log file.

2.3. Evaluation of Measured Data

Besides the data, which can be acquired directly with the used sensors, it is possible to determine further important variables and parameters:

The first is the ethanol mass flow $\dot{m}_{eth}$, which is the product of the measured volume flow $\dot{V}_{eth}$ and the density of the ethanol ρ_{eth}. In order to determine the density, the ambient temperature is used.

$$\dot{m}_{eth} = \rho_{eth} \cdot \dot{V}_{eth} \quad (1)$$

The thrust coefficient C_F is defined as the amplification of thrust due to the gas expanding in the supersonic nozzle compared to the thrust that would be exerted if the chamber pressure acted over the throat area only [3]. Therefore it describes the expansion properties and design quality of the nozzle. With the achieved thrust F, the combustion chamber pressure p_c and the throat area A_t it can be determined as follows:

$$C_F = \frac{F}{p_c A_t} \quad (2)$$

The characteristic velocity c^* is basically a function of propellant characteristics, combustion chamber design and independent of nozzle characteristics. Therefore it is useful for propellant combustion and combustion chamber

design [3]. Knowing the overall propellant mass flow $\dot{m}$, it can be determined with:

(3) $c^* = \frac{p_c A_t}{\dot{m}}$

The specific impulse I_{sp}, describing the overall performance of the rocket engine is defined as:

(4) $I_{sp} = \frac{F}{\dot{m}\, g_0} = \frac{C_F\, c^*}{g_0}$

The heat flow $\dot{Q}$, transferred from the hot combustion gases to the chamber walls can be determined by measuring the coolants increase of temperature ΔT and mass flow $\dot{m}_c$ and using c_p, the mass specific heat.

(5) $\dot{Q} = c_p \cdot \dot{m}_c \cdot \Delta T$

3. COMBUSTION CHAMBER DESIGN

Before the design process of the combustion chamber could be started, some boundary conditions had to be established. We decided that the nominal thrust F of the rocket engine shall be 500 N with a chamber pressure p_c of 15 bars absolute. Furthermore, the oxidizer fuel ratio was chosen to be 1:1. This results in a slight performance decrease but also a huge reduction of the combustion temperature from 3200 K below 2800 K, making the chamber cooling less ambitious. This set of pressure and fuel parameters was used to begin the designing process. The complete parameter set used for the combustion chamber design is given in TAB 1.

Parameter	Value
Thrust F	500 N
Chamber pressure P_c	15 bars
Propellant mass flow $\dot{m}$	250 g/s
Specific impulse I_s	205 s
Firing time	20 s
Oxidant / Fuel ratio (O/F)	1:1
Chamber temperature T_c	2757 K
Char. velocity c^*	1535 m/s
Expansion ratio ε	3

TAB 1. Design Parameters of the Rocket Engine

3.1. Fluid Flow Design

In order to keep the rocket engine as simple as possible, it consists of a cylindrical combustion chamber and a simple cone nozzle.For the design of the nozzle, particularly the exit to throat area ratio and the throat and exit cross sectional area, an ideal rocket propulsion system was used. Here it is possible to express the basic thermodynamic principles as simple mathematical relations which describe a quasi-one dimensional nozzle flow [3]. Introducing a constant Γ, which is a function of the specific heat k:

(1) $\Gamma = \sqrt{k\left(\frac{2}{k+1}\right)^{\frac{k+1}{k-1}}}$

and assuming an optimum expansion, the throat area A_t and the exit to throat area ratio ϵ can be determined by [4]:

(2) $A_t = \frac{F}{p_c}\left[\Gamma\sqrt{\frac{2k}{k-1}}\sqrt{1-\left(\frac{p_a}{p_c}\right)^{\frac{k-1}{k}}}\right]^{-1}$

(3) $\varepsilon = \frac{A_e}{A_t} = \Gamma\left(\frac{p_a}{p_c}\right)^{-\frac{1}{k}}\left\{\frac{2k}{k-1}\left[1-\left(\frac{p_a}{p_c}\right)^{\frac{k-1}{k}}\right]\right\}^{-\frac{1}{2}}$

With F being the intended thrust of the engine, p_a the ambient pressure and p_c the stagnation pressure within the combustion chamber.

The length of the combustion chamber was designed with the help of the characteristic chamber length L^*, which is the length that a chamber of the same volume would have, if it were a straight tube and had no converging nozzle section.

(4) $L^* = V_c / A_t$

Where V_c is the chamber volume up to the throat area [3]. Typical values of L^* for rocket engines working with LOX and ethanol are between 2.5 and 3 m [5]. In order to design a new thrust chamber, it is possible to use those values as a starting point. In order to adjust the length of the combustion chamber it is necessary to run several combustion tests with different lengths [5]. Therefore it is planned to build a thrust chamber consisting of different segments: one nozzle segment and several cylindrical segments for building the combustion chamber. The designed contour of the rocket engine is shown in FIG 3 and the values of the geometry parameters are given in TAB 2.

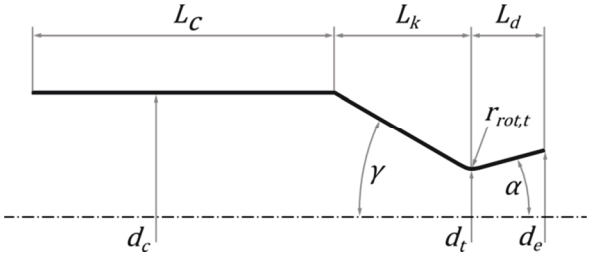

FIG 3. Thrust Chamber Contour

Parameter	value
d_c	65 mm
d_t	18 mm
d_e	30 mm
α	15°
γ	30°
$r_{rot,t}$	18 mm

L_k	44.5 mm
L_d	25.5 mm
$L_c(L^*)$	185 mm (L^* = 2.5 m)

TAB 2. Parameters of the 500 N Thrust Chamber

With this contour and the assumption of an ideal, one-dimensional gas flow it is possible to determine the Mach number, the pressure and the temperature development. A display of the gas state within the rocket engine is given in FIG 4.

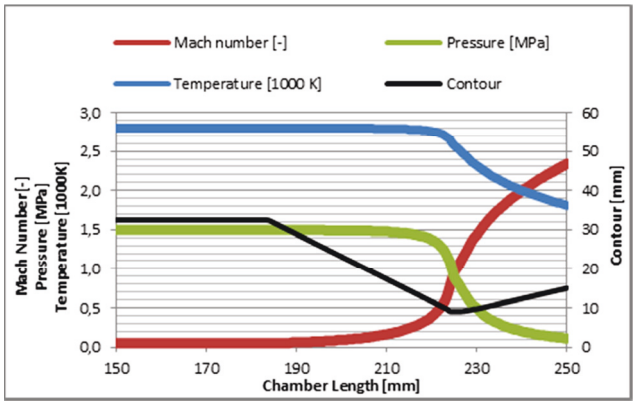

FIG 4. Combustion Gas Properties

3.2. Injector

No component has a bigger influence on the performance characteristics of the combustion chamber than the injector. Each and every per cent loss of efficiency affects the engines specific impulse directly. The injector's task is to mix and atomize oxidant and fuel to achieve a complete combustion of the propellants. Another requirement is to decouple the feeding system from combustion chamber vibrations.

The chosen injection concept is the coaxial swirl injection, at which the propellant components stream axial and parallel to each other into the combustion chamber. Hereby, the propellants are induced tangentially to the circumference of the coaxial element. In doing so, a spin is induced into the fluid flow, so that the stream lies alongside the injector wall due to the centrifugal forces. The propellant mixing takes place inside the injector. That reduces combustion space, which other injection concepts need for mixing. The fluid atomization is an effect of different relative velocities between fuel and oxidant. Both are mixed and atomized by shear and friction forces. Coaxial swirl injectors are the state of the art and the most utilized injectors for Liquid Rocket Engine (LRE) because of its high mixing and atomization properties.

During the SMART Rockets Project two coaxial swirl injectors have been developed and tested, one for 100 N and one for 500 N thrust. The first manufactured injector is shown in FIG 5. The design of the injectors where iteratively improved during a couple of test campaigns with different fluids (Water, liquid Nitrogen, Ethanol and LOX). The main feature of the SRP test injector is the adjustable LOX nozzle which is the inner nozzle of the coaxial injector. It enables to test different mixing scenarios considering the position of the outlet planes of inner and outer nozzle. The effect of the adjustability was well visible at open combustion tests. The flame colour and flame position behind the injector outlet changed depending on the different injector positions. In further tests with the test combustion chamber, it will be possible to measure the thrust and combustion temperature with different injector settings with the goal to find the ideal coaxial injector set-up.

FIG 5. Coaxial Test Injector in Parts [6]

3.3. Test Combustion Chambers

This section covers the very heart of the recent experiments: the test combustion chambers and their nozzle. While the first combustion experiments were conducted without chamber and nozzle, the following tests focused on material behaviour at these harsh conditions during the projected duration time. These material tests covered Oxide-Oxide Ceramic Matrix Composites (OCMC) as well as graphite and phenol liners. For determining the heat loads for the chamber and nozzle materials, a specifically designed metallic test combustion chamber is currently manufactured.

3.3.1. OCMC Flame Tube

With combustion temperatures of 2500 K and above, the material selection and a suitable cooling method is crucial. Metals capable of withstanding such high temperatures are usually heavy and expensive and still need a rather complex cooling system, e.g. regenerative cooling. Wehner [7] investigated the potential of OCMCs as a combustion chamber material. The used OCMC, mainly Al_2O_3 and ZrO_2, promised good results due to its melting point of 2000 °C and a fatigue endurance limit of 1300 °C, which might allow a simple and low weight radiation cooling. Furthermore, due to its oxide components, it cannot degrade from contact with LOX or the ambient air. The downside of this material is its porosity. Needed for its damage tolerant properties, the porosity might be difficult for pressurized vessels such as combustion chambers. This issue is intended to be solved with a glazing, which shall preserve the damage tolerance, while sealing the pores. A first handmade prototype is shown in FIG 6.

FIG 6. OCMC Rocket Engine Prototype [7]

3.3.2. Steel Chamber for Inlay Tests

Because of the complexity of a regenerative cooled liquid rocket engine, additional combustion chamber concepts are examined in the Smart Rockets Project. The first combustion tests shall be done with ablative cooling inlays. Therefore a high grade steel casing with temperature sensors was developed (FIG 7). With the casing it is possible to test different ablative inlays. Currently two types of inlays have been manufactured. One inlay consists of a special high density, high temperature graphite and the other of a phenolic-resin composite. In order to prevent a melting of the steel case, the temperature of the casing will be measured using high temperature thermal elements. Furthermore, the inlays are fabricated in two separate parts; the first has a simple cylindrical shape, while the second forms the nozzle part. The idea is to have replaceable sections, which might be degraded by corrosion and a combination of both inlay materials can be tested in the future. Very promising seems the use of a phenolic-resin cylinder with a graphite nozzle.

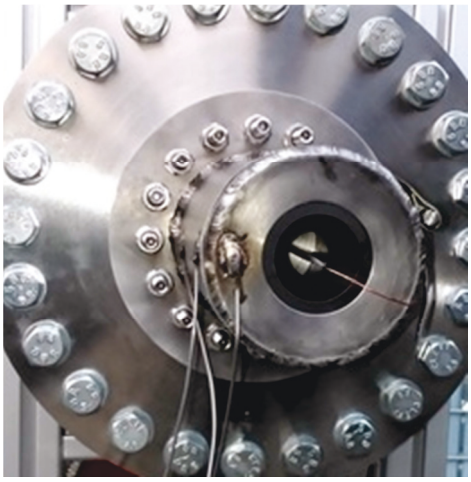

FIG 7. Steel Casing with Graphite Inlays

3.3.3. Test Combustion Chamber

In order to achieve a reliable ignition and a stable combustion, extensive tests are necessary. To study and optimize the combustion process, a test combustion chamber was developed. It shall provide the possibility to determine and influence characteristic combustion parameters such as pressure, temperature and heat fluxes while running at different operating points with a chamber pressure up to 25 bars and a temperature up to 3000 K.

In order to perform combustion tests with different characteristic lengths, the test combustion chamber shall be built of several different segments. FIG 8 shows an exploded view of the test combustion chamber. It consists of a nozzle segment and two cylindrical segments of different length.

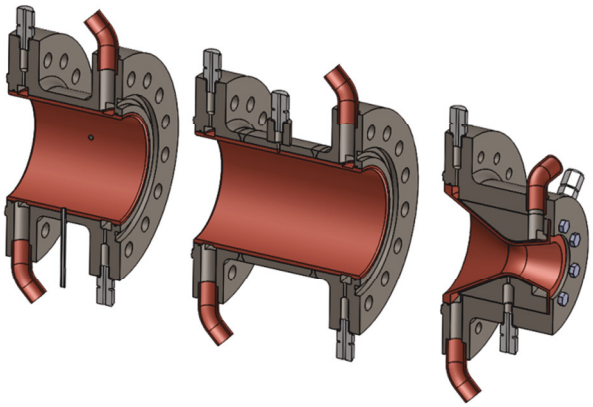

FIG 8. Test Combustion Chamber (Exploded View)

In order to protect the chamber and nozzle walls from overheating and to ensure that the engine endures a high amount of cycles, the test combustion chamber is cooled with water. Therefore, the segments are made of a copper inlay with cooling channels milled into it. To seal these cooling channels, a stainless steel casing surrounds each inlay. These casings are equipped with connection flanges which link the different sections and also provide the connections for the coolant supply.

Alongside the test combustion chamber a variety of different sensors will be mounted. Those are: several temperature sensors for measuring the coolants temperature and determining its temperature rise, temperature sensors measuring the wall temperature and pressure sensors for measuring the pressure within the combustion chamber.

To ensure a safe and reliable function of the test combustion chamber, a structure analysis has been conducted with the ANSYS Workbench software. For this purpose, a static-thermal analysis has been coupled with a static-mechanical analysis, which enables the utilization of the determined temperature distribution as boundary conditions for the mechanical analysis in order to calculate the thermally induced stresses. FIG 9 depicts the temperature field for the maximum operation mode (25 bars, 3000 K). The high thermal conductivity of the inlay material leads to a homogeneous temperature distribution within the cylindrical combustion space, whereas the highest temperatures occur in the nozzle throat. The dimensioned cooling system is able to keep the temperature of the inlay below the working temperature of 770 K.

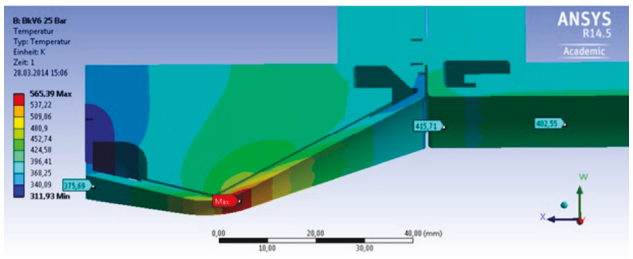

FIG 9. Temperature Distribution for Maximum Heat Load at 25 bar Chamber Pressure

The structural design of the test combustion chamber was successively optimized by mechanical analysis. The integration of expansion spaces for the inlay led to a reduction of the stresses in the flange areas below the yield strength of the material. Hereupon, the maximum stress occurs in the minimum cross-sectional area and exceeds the yield strength of the material. The contour plot of the effective stress distribution for the maximum operation mode is depicted in FIG 10. However, the nozzle structure can hardly be optimized further. A reduction of the wall thickness is needed to reduce the thermal stresses, but leads to an undercut of safety against pressure loads. Another possibility is the reduction of the heat load itself. A lower combustion pressure brings lower strains. On the other hand, an increase of the nozzle throat diameter could lead to a more widely spread distribution of the heat load.

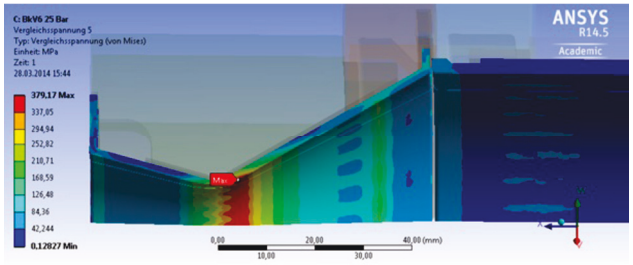

FIG 10. Maximum Thermal Stress in the Copper Inlay

The copper alloy inlay has a tensile strength of 690 MPa at the temperature of operation, which does not get exceeded in any load case. During the operation at pressures of 15 bars and higher, small ductile deformations in the nozzle throat have to be expected. But these are in a sub millimetre range. Test series with the inlay material have been conducted at similar conditions and endurance strength of up to 2900 cycles until structural break-down was concluded.[8]

An estimation of the durability of the designed test combustion chamber also was conducted. For this estimation, the Manson universal slopes equation was used. It includes the tolerable mechanical expansion until deformation sets in on the one hand and the capacity expansibility up to fracture. Thereupon, the creep limit and the breaking elongation are compared with the thermal elongation, which correlates with the operation temperatures. Thus the life span increases with lower temperatures. This is also the case for materials with high breaking elongation, a low E-modulus and high yield strength. For CW106C (Copper Alloy) a breaking elongation of 12 % was chosen, which allows a conservative evaluation of cycling capability. With respect to the material, breaking elongations of up to 40 % can be achieved even at high operation temperatures [9]. The thermal expansion can be derived from the maximum temperatures in the inlay wall, which have been determined for pressures of 3, 15 and 25 bars with thermal analyses. The consequential numbers of cycles until structural failure are listed in TAB 3. These rather conservative estimations show that the test combustion chamber should be capable of resisting the expected loads during the projected life time.

Pressure [bar]	Nozzle throat temperature [K]	Cycles until structural failure
3	351	1,4*10^6
15	463	3400
25	573	700

TAB 3. Lifetime Prediction for different Load Cases

4. MEASUREMENTS

This chapter is dedicated to the presentation of recent experiments. These experiments are used to succeed in the development of the whole rocket engine design, especially fluid system, injector, combustion chamber and nozzle. First flow rate tests with water date back to the end of 2012, while recent experiments were conducted in July and August 2014.

Hence, this chapter starts with experiments focusing on the injector, starting with flow rate tests using different media. They are followed by open combustion tests investigating certain aspects of the mixing and flame distribution. Another test is concerning the type of ignition. Here, a safe and repeatable way of igniting the rocket engine is of interest. A first material experiment has been conducted with an OCMC flame tube, in which the chamber form and therefore also the combustion process are converging towards a rocket engine.

4.1. Flow Rate Tests

We started with the flow through characterization of the injector with water. Under the assumption, that a simple adaption of the results by replacing the fluid density would deliver the needed mass flow, we optimized both injector nozzles. The ethanol nozzle delivered the design mass flow from the beginning, so no further investigations were made.

In order to find the right in- and outlet diameters for the LOX injector, a parameter study was conducted using water. A parameter set with an equal mass at the same pressure level had to be found in order to ensure the O/F of 1:1. For convenience, the mass flow coefficient μ is used for fluid independent characterization. It is the quotient of measured mass flow $\dot{m}$ and expected mass flow following from the Bernoulli equations calculated from the inlet area A_{in}, the pressure drop over the injector p_{inj} and the fluid density ρ:

$$\mu = \frac{\dot{m}}{A_{in} \cdot \sqrt{2 \cdot p_{inj} \cdot \rho}} \quad (5)$$

While the results for water and ethanol were very stable and repeatable, tests with liquid nitrogen (LN2) and LOX were totally different. The water tests resulted in a stable mass flow coefficient of 0.31 for the LOX nozzle. With LN2 and LOX it was quite a challenge to obtain reliable results.

This is caused by local evaporations of the cryogenic fluids within the pipeline which create a transient flow resistant, reducing the mass flow. This problem occurred only with tank pressures below 10 bars and without pre-cooling of the LOX pipeline and injector.

An example of the measurements is given in FIG 11. It shows a test with a tank pressure of approximately 6 bars. The interesting result is the continuously increasing mass flow, while the pressure at the injector is falling. At time index 255 s it seems to level out at first but increases further. Using the measured density of the LOX (1080 kg/m³), the mass flow coefficient increases to 0.40 at the end of this test. This is surprisingly higher than the result obtained with the water tests. This long time transient behaviour of our system might cause an enormous challenge in order to provide enough thrust at the beginning of the flight. On the other hand, the flow tests at higher pressure levels became stationary much faster, after approximately 12 s, which might be enough. Additionally, the LOX pipeline of the test bench is with 2 meters from tank to injector a magnitude longer than projected within the rocket. Hence, the pipeline to cool down will be much shorter and the heating influence smaller. Further investigations have to follow.

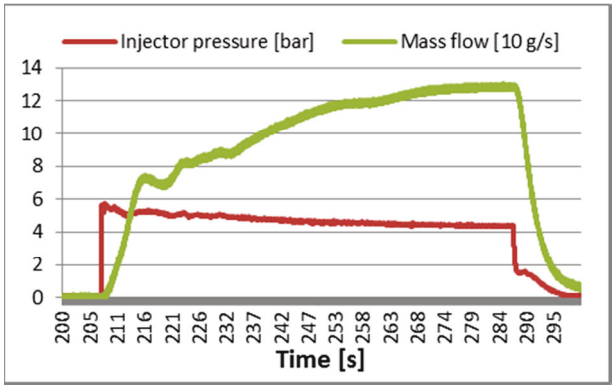

FIG 11. LOX Flow Results

4.2. Open Combustion Tests

At the end of July 2014 a huge milestone of the project could be completed. Within the few days of our first test campaign, we investigated the influence of the test bench and injector parameters, such as the recess position of the LOX nozzle with respect to the ethanol nozzle within the injector. Furthermore, the impact of changing the tank pressure and consequently the pressure drop at the injector as well as the mass flow of the propellants were of interest.

Fast evaluations of the tests were made right after their conduction, considering flame distribution and stability as well as measured mass flows. Subsequently, the pressure settings were adjusted as appropriate. FIG 12 to FIG 15 show a selection of open combustion tests and their results. During the test campaign, all combustion tests were consecutively numbered, which shall be kept here for reference purpose.

FIG 12 shows the first combustion test of the SRP. Without any precooling of the LOX pipeline the oxidizer/fuel ratio (O/F) was very low (0.16), even though the injector pressures of both lines were very similar (LOX: 6.2 bars; Ethanol: 5.9 bars). The combustion itself was stable, where only a small amount of the ethanol interacted with the LOX (small blue flame) and all the rest with the ambient air.

FIG 12. Test #1 First Shot

A completely different flame picture shows FIG 13. The LOX spray cone widens up and captures the ethanol cone, due to a slightly increased injector pressure on the LOX side (7.7 bars and 6.8 bars for Ethanol). Here, the flame was far away from the injector plate, as it is in the test above. This is a result of the recess position of 2.95 mm.

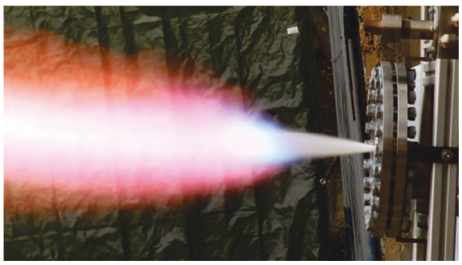

FIG 13. Test # 3 Oxygen Excess

From Test #7 (see FIG 14) on, we tried a different recess position of 3.9 mm. The first obvious thing is the blue flame right at the injector plate, which means that the propellants are mixed within the injector. This test showed a strong pulsating behaviour, since the LOX injector pressure (6 bars) was much higher than the ethanol (4.0 bars). Even though, the O/F of 0.78 was close to the desired state, the instable flame induced an increase of the tank pressures.

FIG 14. Test # 7 Pulsating Combustion

The most promising test was #10. After an extensive cooling of the LOX pipeline and injector pressures of both 6.7 bars, a satisfying stable combustion was established. We realized mass flows of 106 g/s (Ethanol) and 107 g/s (LOX) – almost the design specification of 125 g/s each – even though at a higher pressure level before the injector (FIG 15). The used parameter set provides a stable combustion of the LOX right on the injector plate, while the residual ethanol forms a clear cone that will serve as a film cooling within the combustion chamber. With this test result, we are convinced of being on the right track towards a working liquid propelled rocket engine.

FIG 15. Test # 10 Near Nominal Conditions

4.3. Ignition Systems

During the first test campaign, we investigated the practicability, the repeatability and the reliability of several ignition methods. These tests covered simple igniters such as sparklers, commercial model rocket solutions as well as a self-designed propane-oxygen-burner, which is presented in detail in [6]. All tested systems are displayed in FIG 16.

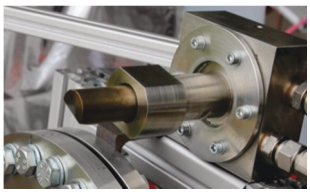

a) Propane-Oxygen-Burner

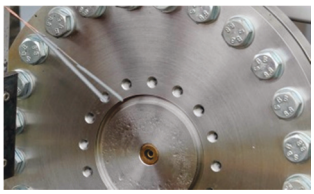

b) Sparkler

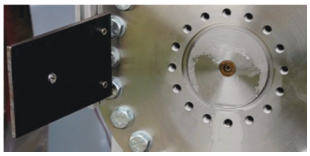

c) Sparking Plug

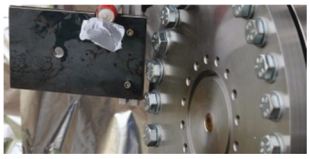

d) Model Rocket Motor

e) Electrical Heater

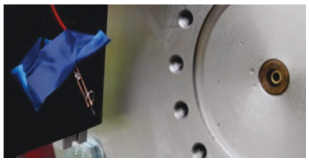

f) Model Rocket Motor Igniter

FIG 16. Experimental Igniters

The propane-oxygen-burner a) (Test #12-16) is used as reference, since all other open combustion tests were conducted with this ignition system. It produces a thermal power of approximately 25 kW [10], which ignites the LOX and ethanol mixture reliably. The propane-oxygen gas itself is ignited via a remote controlled sparking plug. The disadvantage is an external ignition of the propellants. Due to its weight, the burner could not be integrated into the rocket.

Another reliable ignition form is the sparkler b) (Test #23-25). It might be used for experiments but prohibits itself for the launch campaign, since it cannot be ignited remotely. But the magnesium might be useful to enhance a smaller ignition spark that could not ignite the propellants by itself.

A sparking plug c) (Test #17/18) itself proved to be reliable as well for open combustions. It can be started remotely and is small enough to be integrated into the rocket. A limiting weight factor would rather be the peripheral electric devices and the integration of the spark plug into the combustion chamber.

The commercial model rocket components d) (Test # 19) and f) (Test # 20-22) failed both to ignite the propellants. Against all intuition, the exhaust gases of the model rocket motor had not enough energy to start the combustion.

A promising ignition system seems to be an electric heater e) (Test #26/27). This heater is usually used for various types of solid state electrolyte gas sensors[8] developed and build at our institute. It uses a thick film printed and sintered platinum resistor on an aluminium oxide substrate and has a working point at a temperature of 820 °C. The power supply was soldered to gold contacts and enclosed with ceramic glue. 6 W of thermal power were used to heat up the substrate. Two tests were conducted successfully during an open combustion, but further investigation must be done for a reliable ignition of a complete rocket motor.

4.4. OCMC Flame Tube

For a first material analysis of the behaviour of OCMC in combustion gases a flame tube was mounted to the test bench. It is made from similar but less expensive material to the one envisaged for the rocket engine, since the flame tube does not have to withstand higher pressure loads. Its contour covers only the cylindrical part of the rocket engine and a flange is used for the connection to the injector plate. The flame tube prior to and after the test can be seen in FIG 17.

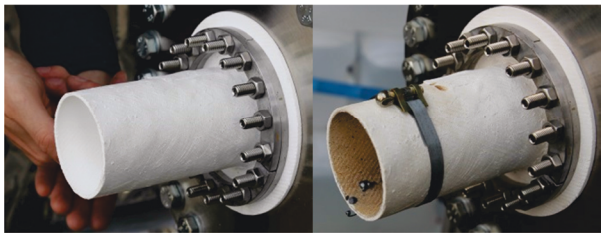

FIG 17. OCMC Flame Tube before and after Testing

Even though no temperature measurement of the flame tube was made during the test, some interesting effects can be analysed from the pictures and the test bench data in TAB 4. It can be seen, that the steel rod of the sparkler melted during the test, indicating a hot gas temperature of 1500 °C or above.

Obvious is the colour change of the OCMC material. On the inside, this could be easily explained with soot agglomeration, due to the fuel rich combustion. For the outside colour change, the porosity could have been responsible. Another explanation could be changes in the material, which have to be investigated. Furthermore, the injector plate has shown first signs of heat tinting, which did not occur during open combustions. So the flame tube had a throttling effect on the combustion gases, which results in an uncritical heat accumulation near the injector plate.

[8] Gas species: atomic and molecular oxygen, ozone, oxides of nitrogen, carbon dioxide [11]

	Test #28	Test #29
$\dot{m}_{LOX}$	36 g/s	33 g/s
$\dot{m}_{Eth}$	44 g/s	49 g/s
$\frac{\dot{m}_{LOX}}{\dot{m}_{Eth}}$	0,82	0,67
$p_{inj,LOX}$	7,6 bar	7,2 bar
$p_{inj,Eth}$	6,5 bar	6,3 bar
t_{burn}	7 s	14 s

TAB 4. Flow Properties Flame Tube Test

5. OUTLOOK

The first basic tests for our combustion chamber development are completed and the detailed analysis of the test results has to be finished. Final conclusions have to be drawn, upcoming tests prepared and further parts, especially the metal test combustion chamber, completely manufactured.

With the metal test combustion chamber, the calculated heat loads for the materials can be actually measured and verified. Furthermore, a full characterization of the rocket engine design is possible, e.g. with respect to the specific impulse or the characteristic velocity.

With all that experience obtained during the first and the upcoming test campaigns, the development of the engine will succeed and the flying rocket becomes more concrete. A full overview of the actual rocket design and all the ground support equipment can be obtained in [2].

6. ACKNOWLEDGEMENTS

We appreciate the assistance and support by: The DLR and the BMWi, who fund the project (Ref.-Nr. 50 RL 1256); Karsten Lappöhn, the manager of STERN; David Kirsten, from Kirsten Engineering for his support concerning LOX during the tests; Bernd Middendorf, a research assistant contributing before and during the test campaign; Maximilian Ehrhardt, Jens Schubert and Johannes Aurich, student assistants, who mainly contributed to the fabrication of the test bench; Frank Wehner, former materials engineering student, who presented first OCMC solutions; Walter Pritzkow, from Walter E.C. Pritzkow Spezialkeramik, for the low priced supply with OCMC; Tilman Schüler, from the research group Small Satellites and Spin-off technologies for his support and supply with ceramic heaters; Martin Brandt, who designed the propane-oxygen-burner; Sebastian Weixler, who completed the injector plate and all other unnamed students and contributors to this project.

7. REFERENCES

[1] **K. Lappöhn, D. Regenbrecht, D. Bergmann, M. Schmid, P. Rickmers**; *STERN - Raketenprogramm für Studenten*; 61. Deutscher Luft- und Raumfahrtkongress; Deutsche Gesellschaft für Luft- und Raumfahrt – Lilienthal-Oberth e.V.; Bonn 2012

[2] **C. Bach, J. Sieder, S. Grasselt-Gille, O. Przybilski, M. Tajmar**; *Proceedings of the SMART Rockets Project: Development of a Sounding Rocket and the corresponding Ground Support Equipment*; 63. Deutscher Luft- und Raumfahrtkongress; Deutsche Gesellschaft für Luft- und Raumfahrt – Lilienthal-Oberth e.V.; Augsburg 2014

[3] **G. P. Sutton; O. Biblarz**; *Rocket Propulsion Elements*; Seventh Edition; John Wiley & Sons, Inc.; 2001

[4] **E. Messerschmid; S. Fasoulas**; *Raumfahrtsysteme*; 3., neu bearbeitete Auflage; Springer-Verlag Berlin Heidelberg, 2009

[5] **M. Barrère; A. Jaumotte; B. F. Veubeke; J. Vandenkerckhove**; *Raketenantriebe*; Elsevier Publishing Company; 1961

[6] **J. Sieder; C. Bach; O. Przybilski, M. Tajmar**; *SMART Rockets – A contribution to the DLR STERN programme by Dresden University of Technology*; 5th European Conference for Aeronautics and Space Sciences (EUCASS), Munich, July 2013

[7] **F. Wehner**; *Einsatz einer oxidfaserverstärkten Oxidkeramik (OCMC) als Werkstoff für Raketenbrennkammern*; Diplomarbeit; Technische Universität Dresden, Institut für Luft- und Raumfahrttechnik; Dresden 2014

[8] **J. B. Conway; R. H. Stentz; J. T. Benling**; *High Temperatur, Low Cycle Fatigue of Copper-Base Alloys in Argon; Part II-Zirkonium-Copper at 482, 538 and 593°C*; National Aeronautics and Space Administration, Cincinnati, 1973

[9] **D. Fulton**; *Investigation of Thermal Fatigue in Non-Tubular Regeneratively cooled Thrust-Chambers*, Final Report Volume 1, Rocketdyne Division, California,1973

[10] **M. Brandt**; *Auslegung, Bau und Testung eines mehrfach verwendbaren Zündsystems für Raketenbrennkammern mit flüssigen Treibstoffen*; Großer Beleg; Technische Universität Dresden, Institut für Luft- und Raumfahrttechnik; Dresden 2012

[11] **S. Fasoulas; T. Schmiel; R. Baumann; M. Hörenz; F. U. Hammer; K. Bockstahler; J. Witt**; *New Miniaturized and Space Qualified Gas Sensors for Fast Response In Situ Measurements*; 40th International Conference on Environmental Systems; DOI: 10.2514/6.2010-6147